Biochimica et Biophysica Acta, 1060 (1991) 159–165

ADONIS 000527289100231B

BBABIO 43492

Spectroscopic studies of the nickel-substituted *Desulfovibrio vulgaris* Hildenborough rubredoxin: implication for the nickel site in hydrogenases

Isabelle Mus-Veteau [1], David Diaz [2], Jesus Gracia-Mora [2], Bruno Guigliarelli [3], Genevieve Chottard [4] and Mireille Bruschi [1]

[1] *Laboratoire de chimie bacterienne C.N.R.S., Marseille (France),* [2] *Departamento de quimica inorganica y nuclear, Facultad de quimica, U.N.A.M. (Mexico),* [3] *Laboratoire d'electronique des milieux condensés, U.R.A. C.N.R.S. 784, Université de Provence, Marseille (France) and* [4] *Laboratoire de chimie des metaux de transition, U.R.A. CNRS 419, Université Pierre et Marie Curie, Paris (France)*

(Received 31 January 1991)

Key words: Rubredoxin; Metal replacement; Nickel-substituted rubredoxin; Nickel coordination; Hydrogenase; (*D. vulgaris*)

An Ni-substituted rubredoxin has been prepared using a new method of metal replacement. The Ni center appears to be constituted by one nickel atom coordinated to four cysteine residues in a distorted tetrahedral geometry. After oxidation, this site gives EPR signals very close to those observed in the Ni-containing hydrogenases. The amino-acid sequences which appear to be involved in the nickel fixation of the substituted rubredoxin show homologies with cysteine-containing motiefs present in the Ni hydrogenase sequences. The different results and observations reported herein are discussed and allow a model to be proposed for nickel coordination in hydrogenases.

Introduction

The role of nickel in biological systems has been considered only recently and a search of the chemical properties of relevant nickel compounds has been undertaken to interpret major unresolved questions concerning the Ni-containing enzymes.

The (NiFe) hydrogenases contain a single atom of nickel per enzyme molecule as well as iron-sulfur clusters as prosthetic groups [1,2]. Some of these proteins also contain a selenium atom, allowing a further subdivision, the (NiFeSe) hydrogenases. Cumulative chemical and spectroscopic evidence suggests that the nickel catalyzes both the reductive formation and oxidative cleavage of dihydrogen [3].

An ESR study of Ni(III) complexes of various sulfhydryl-containing peptides has suggested the involvement of at least one cysteine sulfur in the hydrogenase Ni center [4]. Nickel extended X-ray absorption fine structure (EXAFS) [5] and X-ray absorption near-edge spectroscopy (XANES) [6] studies propose that this atom is coordinated to approximately four sulfur atoms in either a distorted octahedral or square pyramidal array. It has been reported by electron spin echo envelope modulation (ESEEM) spectroscopy experiments that a ^{14}N, possibly from imidazole, would be involved in the Ni coordination [7]. Remarkably, the redox potentials for the Ni(III)/Ni(II) couple of these hydrogenases occur in the range of -150 to -400 mV versus normal hydrogen electrode (NHE), which is in striking contrast with the more positive values, around 1 V, reported on the Ni(III)/Ni(II) couple of classical coordination compounds [8,9].

In synthetic complexes, the higher oxidation states of Ni can often be stabilized by anionic polarizable ligands containing deprotonated amides or oximes [10] which contribute to lower the redox potential. Thiolates being polarizable ligands, recent research activity has been directed at elucidating the structural, reactivity and physical properties of nickel thiolate coordination complexes as models of Ni centers in hydrogenases.

To understand the structure–function relationships of active sites in metalloproteins, core extrusions of metal centers [11] and transition metal replacement at

Correspondence: M. Bruschi, Laboratoire de chimie bacterienne C.N.R.S., 31 chemin J. Aiguier, B.P. 71, 13277 Marseille Cedex 9, France.

redox-proteins active sites have been realized. As an example, the native iron atoms in rubredoxin from *Pseudomonas oleovorans* were replaced by cobalt to give rubredoxin containing two atoms of cobalt per protein molecule [12]. Recently, the iron atom has been replaced by a nickel in the *Desulfovibrio gigas* rubredoxin, the product obtained has been studied by UV-visible absorption, variable-temperature magnetic circular dichroism (MCD) spectroscopies [13] and its reactivity in the deuterium–proton exchange reaction and in H_2 production has been tested [14].

Rubredoxins are non-heme iron proteins involved in electron transfer processes. They contain a single iron atom chelated to a polypeptide chain of 6000 Da by four cysteinyl sulfur atoms in a distorted tetrahedral coordination [15–17]. The highly refined models of crystalline rubredoxins from *C. pasteurianum* [18], *D. vulgaris* [19] and *D. gigas* [20] have been derived from X-ray diffraction data. The active sites of these proteins have been well characterized and their properties make rubredoxins valuable candidates for metal center substitution experiments.

In an attempt to obtain a model for the Ni site of hydrogenases, we have synthetized a nickel-substituted *Desulfovibrio vulgaris* Hildenborough rubredoxin using a new method of iron atom replacement with a Ni complex. The chemical and spectroscopic properties of the Ni derivative are reported.

Experimental procedure

Preparation of the Ni-substituted rubredoxin. The conditions for growth of *D. vulgaris* cells and isolation of rubredoxin were previously described [21].

The Ni-synthetic analogue has the experimental formula $[Ni(SPh)_2]$ and was prepared by the general method reported [22,23]. The calculated elemental analysis was C: 52.04% and H: 3.61% and encountered is C: 50.0% and H: 3.5%. The molar electrical conductivity measured in dimethylformamide (DMF) solution and at room temperature, was 20.21 ohm^{-1} cm^{-1}, indicating that it is a non-electrolyte complex. The value of the effective magnetic moment (μ_{eff}) for this complex is 2.84 μ_B and was obtained in a Johnson Matthey magnetic susceptibility balance at room temperature. This μ_{eff} value is in agreement with a tetrahedral environment for the nickel atom.

The electronic absorption spectrum was recorded in the region from 800 to 260 nm in DMF solution at 25 °C. The spectrum presents absorption bands reported in Table I. This region is dominated by relatively intense absorptions, most or all of which appear to arise from S → Ni charge transfer excitations.

The protein (1 mg/ml) was dissolved in a solution of 0.05 M Tris-HCl buffer at pH 7.6 (20%) and DMF (80%). The proteinic solution was added to a mixture of 100-excess of thiophenol and 120-excess of triethylamin. The apoprotein thus obtained exhibited no visible absorbance, indicating the loss of iron chromophores. After the immediate extrusion of iron atoms, 10-excess of pure Ni synthetic complex $[Ni(SPh)_2]$ in DMF solution were added to the mixture to reconstitute the rubredoxin. *G10 Sephadex*, preequilibrated with H_2O was used to purify the Ni derivative. The Ni-substituted rubredoxin (Ni–Rd) and the synthetic analogue complex were studied spectrophotometrically from 800 nm to 260 nm (Hewlett Packard 8452 A Diode Array spectrophotometer coupled to a Hewlett Packard Vectra QS/16S – computer Philips PU 8820 UV/Vis spectrophotometer).

Nickel analysis. The Ni-content in the Ni–Rd was determined by an Unicam model SP1900 atomic absorption spectrometer. A solution of $Ni(NO_3)_2$–$6H_2O$ in the same buffer as the protein was used as standard.

Circular dichroism spectroscopy. CD measurements have been carried out on a J.Y. Mark IV Dichrograph at room temperature.

NMR spectroscopy. NMR samples consist of about 2 mg of the lyophilized protein dissolved in 0.3 ml of ^2H_2O containing 0.1 M phosphate buffer. The pH of the sample was adjusted to the desired value by addition of 0.1 M NaO^2H or 0.1 M ^2HCl from a micrometer syringe with rapid stirring.

Reduction of the protein was carried out by addition of 2 excess of solid sodium dithionite to the solution. ^1H-NMR spectra were recorded in the Fourier mode on a Bruker AM200 spectrometer. Chemical shifts are in parts per million (ppm) from internal CCl_4 tetramethylsilane (TMS). DHO signal was suppressed by a presaturation pulse from the decoupler.

EPR spectroscopy. The EPR spectra were recorded on a Bruker ESP 300 spectrometer equipped with an ESP 1620 data-processing unit. The temperature of the sample was maintained at 10 K with an Air-Products Helitran helium gas-flow system. We used oxidized rubredoxin solutions of 0.5 mM concentration in 0.1 M PO_4 buffer (pH 7.6). The oxidation of the Ni-substituted rubredoxin sample was carried out by addition of 1 equiv. of potassium ferricyanide.

Results

Optical spectral properties

The *D. vulgaris* Ni-substituted rubredoxin was prepared in aerobic conditions. It contained one Ni atom per molecule of protein and had a characteristic yellow color. It exhibited absorption bands in the visible region at 360 nm and 450 nm (Table I) attributed to the S → Ni(II) charge transfer transitions. Two weaker bands can be observed at 660 nm and 720 nm which arise from Ni(II) *d–d* transitions. These spectroscopic characteristics are in good agreement with those previ-

ously published on the Ni-substituted aspartate transcarbamoylase [24] and on the Ni-substituted *D. gigas* rubredoxin [13]. They indicate an approximately tetrahedral coordination of the nickel atom in the Ni–Rd.

Circular dichroism spectroscopy

The superposition of the CD spectra of both the native and the Ni-substituted rubredoxins in the three main regions is shown in Fig. 1. These domains are assigned to the sulfur–metal charge transfer transitions in the 300 to 800 nm region (Fig. 1a), to the aromatic residues transitions in the 250 to 300 nm region (Fig. 1b) and to the polypeptide transitions below 240 nm (Fig. 1c). In the visible part of the spectrum (Fig. 1a), the absorption bands of native rubredoxin at 375 nm and 490 nm are ascribed to charge transfer transitions from cysteine sulfur orbitals to the d_π and d_σ orbitals of iron. Both bands are split in the Ni-substituted rubredoxin spectrum, revealing a lowering from the ideal Td symmetry of the FeS_4 core. In the aromatic region (Fig. 1b), native and substituted rubredoxins exhibit a strong absorption at 278 nm, whereas their CD spectra are markedly different: the main negative CD band of the native protein (located at 268 nm) disappears upon substitution, the fine structure elements being conserved. Based on literature data [25], it seems possible to assign the 292 nm (and 283 nm in part) negative peak to the single tryptophan residue, the phenylalanine residues being mainly responsible for the 268 nm main CD. The observed changes would suggest that the tryptophan residue remains unaffected by the metal substitution.

The intrinsic CD is composed of two negative bands at 220 nm and 200 nm (Fig. 1c). Taking into account their shape and position, the 220 nm band has been ascribed to the β structure. The metal substitution leads to a decrease of the intensity of this band, suggesting a less ordered structure for the Ni derivative.

NMR spectroscopy

The 200 MHz ^{1}H-NMR spectra of both oxidized and reduced *D. vulgaris* Hildenborough rubredoxin (Fig. 2a and 2b) look like those previously published for *C. pasteurianum* [26] and *D. gigas* [27] rubredoxins. The Fig. 2c presents the ^{1}H-NMR spectrum of the oxidized Ni-substituted rubredoxin. This spectrum re-

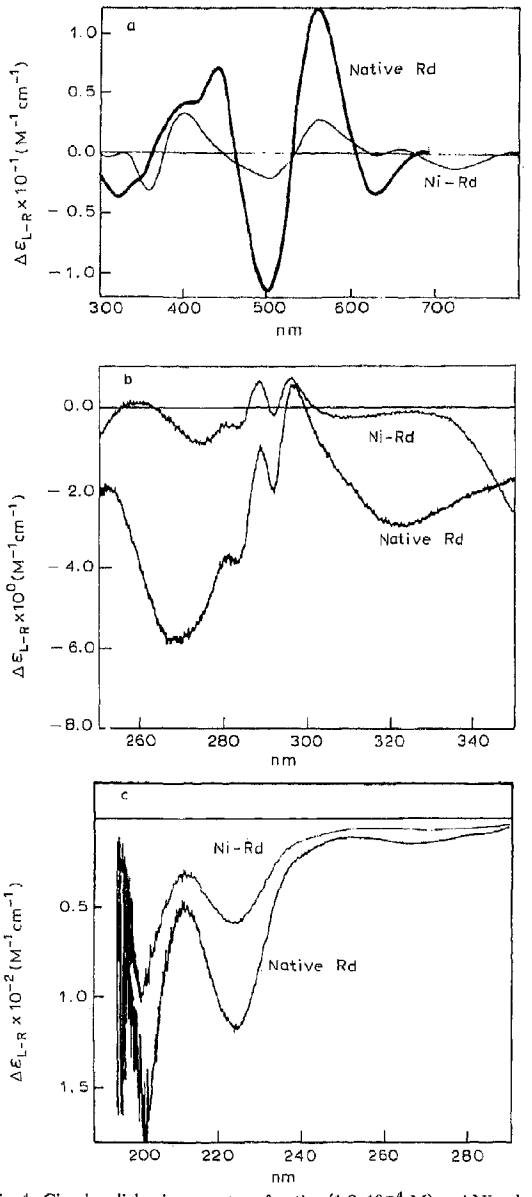

Fig. 1. Circular dichroism spectra of native ($1.8 \cdot 10^{-4}$ M) and Ni-substituted ($3.7 \cdot 10^{-4}$ M) rubredoxins in 0.1 M phosphate buffer at pH 7.6. Pathlength: 5 mm (a and b), 1 mm (c).

TABLE I

Absorption values (λ) and molar extinction coefficients (ε) of Ni complex, native and Ni substituted rubredoxins

	Native *D. vulgaris* Rd		[Ni (SPh)$_2$]			Ni–Rd	
λ (nm)	493	380	472	342	300	450	360
ε (M^{-1} cm^{-1})	6966	4139	5541	6853	7536	2700	5000

veals many new resonances in the region from 380 to −30 ppm [28]. In the very low-field region, eight peaks are observed between 380 and 150 ppm. Similar isotropically shifted resonances have been observed for a series of alkylthiolate-Fe(II) complexes: $[Fe(SR)_4]^{2-}$ [27]. These resonances are all assigned to coordinated sulfur methylene hydrogens β and hence correspond to the βCH_2 groups of coordinated cysteinate in reduced *D. gigas* rubredoxin. Therefore, the eight peaks of the 380 to 150 ppm region of the Ni–Rd spectrum could be assigned to βCH_2 hydrogens of cysteinate ligands to Ni(II). These spectral properties indicate that the nickel atom is coordinated by four cysteine residues in a tetrahedral geometry.

The resonances between 30 and −30 ppm could be assigned to αCH hydrogens of cysteinate ligands to Ni(II), to aromatic residues and methyl group hydrogens very close to the nickel center.

EPR spectroscopy

In the oxidized state, native *D. vulgaris* Hildenborough rubredoxin presents an EPR signal with g values

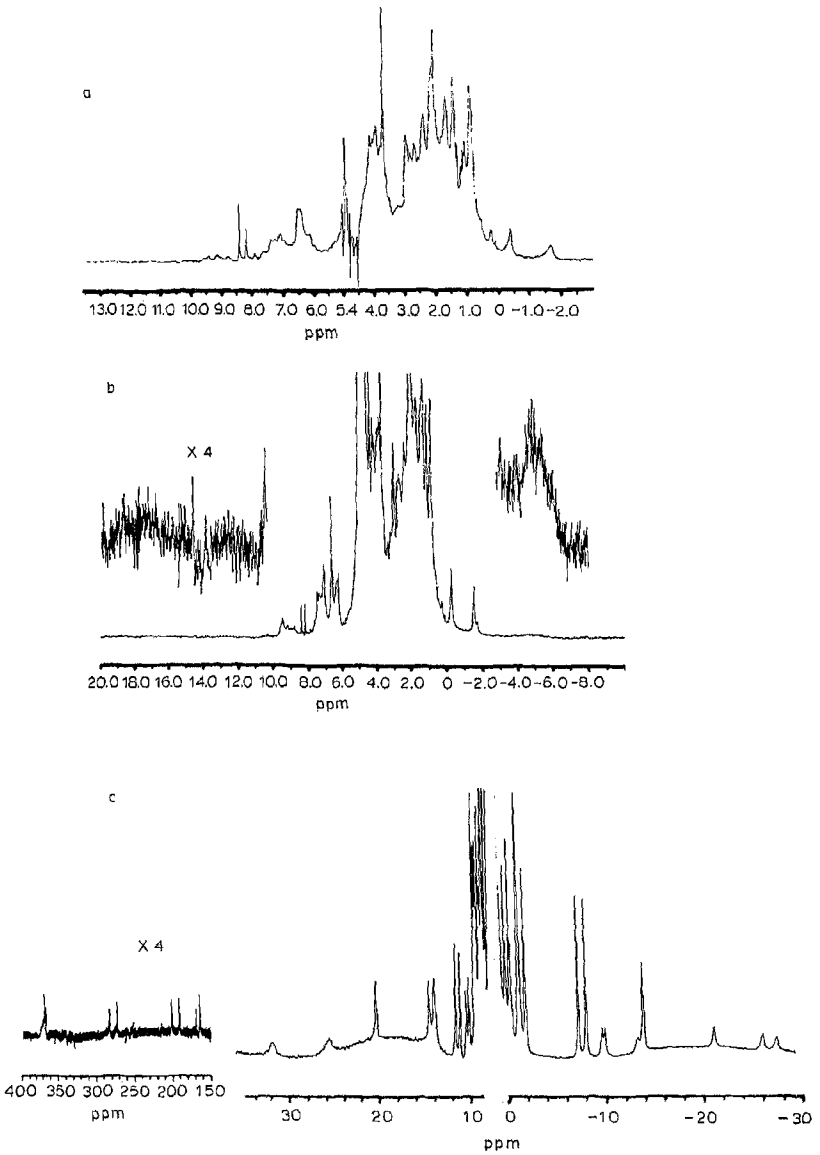

Fig. 2. ^{1}H-NMR spectra of native oxidized (a), native reduced (b) and oxidized Ni-substituted (c) *D. vulgaris* Hildenborough rubredoxins. The spectra were recorded at 20 ° C and the rubredoxin concentrations were 1 mM, in 0.1 M phosphate buffer at pH 7.8.

around 9.4 and 4.3 characteristic of a high-spin Fe(III) ion in a distorted tetrahedral environment of sulfur atoms.

As prepared, the Ni–Rd is EPR-silent; this results from the Ni(II) state of the nickel ion in the substituted protein [13]. No Fe(III) signal can be detected, which means that the solution obtained after the purification on G10 Sephadex contains no residual native Fe–Rd. After oxidation of the sample by addition of one equivalent of potassium ferricyanide, a rhombic EPR spectrum develops, with g values at 2.285, 2.105 and 2.038 (Fig. 3). Ni ions can occur with oxidation states ranging from Ni(0) to Ni(III). The Ni(II) state is found in a majority of the complexes, the other states being less common due to their lower stability. The Ni(I) ($S = 1/2$) and Ni(III) ($S = 1/2$ or $3/2$) oxidation states are EPR active and they are immediately distinguishable from Ni(0) ($S = 0$) and Ni(II) ($S = 0$ or 1) which are EPR-silent.

The detection of Ni EPR signals in biological systems was first reported by Lancaster in 1980 [29] in hydrogenase preparations of *Methanobacterium bryantii*. This signal, attributed to Ni(III), shows rhombic features at around $g = 2.3$, 2.2 and 2.0, and has now been observed in the oxidized states of many hydrogenases (Table II). The comparison of the g values of ferricyanide oxidized Ni–Rd with those reported in

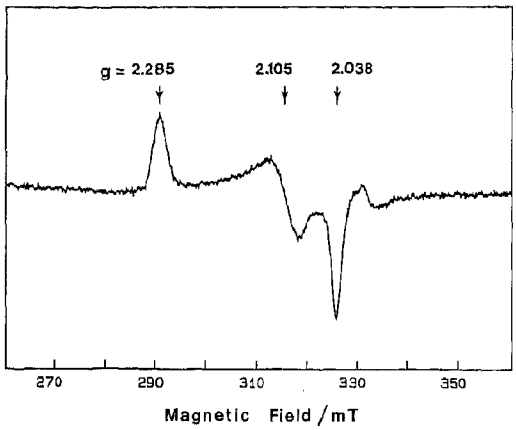

Fig. 3. EPR spectrum of Ni-substituted *D. vulgaris* Hildenborough rubredoxin oxidized with ferricyanide. The sample concentration was 0.5 mM. The spectrum was recorded with the following experimental conditions: temperature, 10 K; microwave frequency, 9.303 GHz; microwave power, 1 mW; modulation frequency, 100 kHz; modulation amplitude, 1 mT.

Table II confirms that the oxidation state of the nickel ion in this protein is Ni(III). This result then indicates that, in the peculiar environment of the Ni atom in Ni–Rd, the Ni(III)/Ni(II) redox potential is suffi-

TABLE II

g values of Ni(III) EPR signals in nickel-containing hydrogenases, Ni(III)-peptide complexes and Ni-substituted D. vulgaris Hildenborough rubredoxin

	EPR g values		
	g_1	g_2	g_3
Ni-containing hydrogenases			
Thiocapsa roseopersicina	2.32	2.23	2.01
Methanobacterium thermoautotrophicum (Marburg)	2.30	2.23	2.01
Desulfovibrio gigas (NCI B9332)	2.31	2.23	2.02
Desulfovibrio desulfuricans (ATCC27774)	2.32	2.16	2.01
Desulfovibrio desulfuricans (Norway 4, soluble)	2.22	2.07	2.01
Desulfovibrio desulfuricans (Norway 4, membrane)	2.32	2.232	2.01
Desulfovibrio multispirans (n. sp.)	2.31	2.22	2.00
Desulfovibrio baculatus (strain 9974)	2.34	2.15	2.00
Methanobacterium bryantii	2.30	2.23	2.02
Methanosarcina barkeri (DSM 8000)	2.24	2.12	2.02
Peptide-Ni(III) complexes			
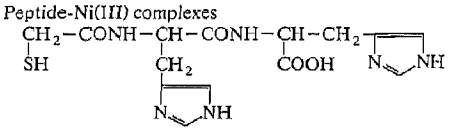	2.26	2.19	2.02
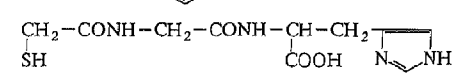	2.27	2.06	2.01
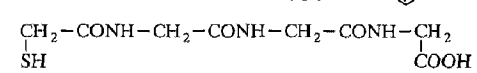	2.27	2.22	2.01
Ni-substituted-Rd			
Desulfovibrio vulgaris Hildenborough (this work)	2.29	2.11	2.04

ciently lowered so that Ni(II) can be oxidized with ferricyanide.

Discussion

A better understanding of the structural features and functional properties of metalloenzymes may be achieved through the knowledge of the physicochemical properties of synthetic active site models and metal center substituted or reconstituted proteins. The previous published core extrusions and metal replacements were carried out using trichloroacetic acid precipitation to obtain the apoprotein and reconstitution under anaerobic conditions with a metal solution [13,14,24]. Here, a new method of metal substitution under mild conditions and without previous preparation of apoprotein is reported. The synthesis of the *Desulfovibrio vulgaris* Hildenborough Ni-substituted rubredoxin has been realized under aerobic atmosphere using the strong affinity of thiophenol for the iron atom to extract the native metal and a nickel complex, $[Ni(SPh)_2]$, in dimethylformamide solution to reconstitute the rubredoxin.

The results given by different analytic and spectroscopic methods show that the substitution of Fe with Ni is effective. The similarities observed between the optical spectrum of Ni–Rd and those of native rubredoxin and Ni complex suggest that in the three cases the metal atom is in a tetrahedral environment of sulfur atoms, in agreement with the results previously published on the Ni-*D. gigas* rubredoxin [13] and the Ni-aspartate transcarbamoylase [24].

The NMR spectrum of the Ni–Rd enables one to affirm that the nickel incorporation at the rubredoxin active site does not affect the folding of the protein. However, the CD spectra show a lowering from the ideal tetrahedral geometry of the active site and a less ordered structure for the Ni derivative.

When oxidized by ferricyanide, the Ni–Rd exhibits an EPR signal characteristic of a low-spin Ni(III) ion ($S = 1/2$) (Table II). A pure tetrahedral symmetry of the Ni(III) ion would lead to a spin state $S = 3/2$ which gives an EPR signal around $g = 4.3$ [30]. We can then conclude that the tetrahedral environment of the nickel atom is probably highly distorted, toward to a square planar geometry as suggested by the rhombicity of the EPR spectrum: $g_z > g_y \simeq g_x$. In the case of a square planar symmetry, the predicted rhombicity of the $\tilde{g}$ tensor corresponds to $g_{\parallel} > g_{\perp}$ [9,30]. The strong lowering of the Ni(III)/Ni(II) redox potential observed by preliminary studies in the Ni–Rd, as in Ni synthetic compounds with thiolate ligands [31], shows that the relative stabilization of the Ni(III) state in hydrogenases is most likely due to the presence of several sulfur ligands.

In their oxidized state, Ni-containing hydrogenases are generally not catalytically active and give two distinct EPR signals of Ni(III), Ni_A and Ni_B [3,32]. On reduction, these signals disappear but another signal, termed Ni_C, can be observed at $g = 2.19$, 2.16 and 2.01 at more negative potentials. This signal has been associated with a metal-hydride species involved in the catalytic cycle of the enzyme. The valence state of the Ni ion in these species (Ni(I) or Ni(III)) is not known [3,33,34] and cannot be determined solely from the EPR data. Upon illumination, the metal-hydride bond is broken and the Ni_C signal is replaced by a Ni_C^* signal with g values at 2.28, 2.12 and 2.03 [3,33]. These g values are very close to those given by oxidized Ni–Rd (2.285, 2.105 and 2.038). This would indicate that the Ni_C^* signal arises from a trivalent Ni ion and could then support previous arguments in favor of an Ni(III)-H species associated with the Ni_C signal [34,35].

In view of these different results, the sequence alignment of the various Ni-containing hydrogenases [36,37] would be helpful to characterize the cysteine residues implicated in the Ni coordination. Ni hydrogenases are composed of two different subunits, a small one of about 30 kDa and a large one of about 60 kDa and contain a redox active nickel and several (Fe–S) clusters [36]. On the basis of this sequence comparison it has been described that the motief Cys_{530}-X-X-Cys_{533}-X-X-His_{536} (*D. gigas* numbering [38]) in the C terminal region of the large subunit could be involved in the coordination of the nickel in both (NiFe) and (NiFeSe) hydrogenases. We propose that the other similar motief in the N terminal sequence of the large subunit (Cys_{65}-X-X-Cys_{68}-X-X-X-His_{72}), which is also highly conserved, could be involved in the binding of the nickel atom. Remarkably, the homology comparison of various rubredoxins [39] reveals the same very conserved motief Cys-X-X-Cys at the N and C parts of the sequence. The cysteine residues of these two clusters are coordinated to the iron atom in the native rubredoxin and to the nickel atom in the Ni substituted one. Taking into account that a stable Ni complex can accept from four to six ligands in the Ni(II) as well as in the Ni(III) state, a tentative structure of the nickel environment in hydrogenases has been postulated [7]. This scheme proposes the involvement of two sulfur atoms from cysteine residues in the (NiFe) hydrogenases or one sulfur atom from a cysteine residue and one selenium atom from the selenocysteine residue in the (NiFeSe) hydrogenases, one nitrogen atom from imidazole and one more ligand, X, for a fourth permanent site, allowing the approach of hydrogen molecules in the course of activation.

In the light of the different results and observations reported herein, another possible scheme for the nickel environment in hydrogenases can be proposed based on the Ni coordination in the Ni-substituted rubredoxin. This model would involve the four cysteine

residues from the two highly conserved Cys-X-X-Cys-X-X-(X)-His sequences of the large (NiFe) and (NiFeSe) hydrogenase subunit as the nickel ligands. The histidine residue observed by ESEEM spectroscopy [7] could more probably be involved in the close environment of the metal atom.

The crystalline structure of hydrogenases being still unresolved, further studies to elucidate the Ni–Rd structure using X-ray crystallography and 2D-NMR spectroscopy would be helpful to determine the nickel coordination.

Acknowledgements

The authors gratefully acknowledge the laboratory of Dr Arréguin (Instituto de quimica, UNAM, Mexico) where this work has been initiated. We thank Dr F. Guerlesquin for invaluable assistance and suggestions, Dr M. Noailly (Service inter-universitaire de RMN, Faculté de Pharmacie, Marseille) for the use of the NMR spectrometer and Prof. P. Bertrand for helpful discussions. Thanks are due to G. Leroy for her assistance in the protein purification and to Dr Laffont (Laboratoire de geologie du quaternaire, CNRS Luminy, Marseille) for the nickel analysis.

References

1 Hatchikian, E.C., Bruschi, M. and LeGall, J. (1978) Biochem. Biophys. Res. Commun. 82, 451–461.
2 Cammack, R., Patil, D., Aguirre, R. and Hatchikian, E.C. (1982) FEBS Lett. 142, 289–292.
3 Cammack, R., Patil, D.S., Hatchikian, E.C. and Fernandez, V.M. (1987) Biochim. Biophys. Acta 912, 98–109.
4 Sugiura, Y., Kuwahara, J. and Suzuki, T. (1983) Biochem. Biophys. Res. Commun. 115, 878–881.
5 Johnson, M.K., Lindhal, P.A., Zambrano, I.C., Czechowski, M., Peck, H.D., Jr, DerVartanian, D.V. and LeGall, J. (1985) Biochem. Biophys. Res. Commun. 128, 220–225.
6 Eideness, M.K., Sullivan, R.J. and Scott, R.A. (1988) in The Bioinorganic Chemistry of Nickel, Ch. 4 and 9 (Lancaster, J.R., ed.), VCH, New York.
7 Chapman, A., Cammack, R., Hatchikian, E.C., McCraven, J. and Peisach, J. (1988) FEBS Lett. 242, 134–138.
8 Lappin, A.G. and Mc Auley, A. (1988) Adv. Inorg. Chem. 32, 241.
9 Jacobs, S.A. and Margerum, D.W. (1984) Inorg. Chem. 23, 1195–1201.
10 Kruger, H.-J. and Holm, R.H. (1987) Inorg. Chem. 26, 3645–3647.
11 Bonomi, F. and Kurtz, D.M. (1982) Biochemistry 21, 6838–6843.
12 May, W.S. and Kuo, J.Y. (1978) J. Am. Chem. Soc. 17, 3333–3338.
13 Kowal, A.T., Zambrano, I.C., Moura, I., Moura, J.J.G., LeGall, J. and Johnson M.K. (1987) Inorg. Chem. 27, 1162–1166.
14 Saint-Martin, P., Lespinat. P.A., Fauque, G., Berlier, Y., LeGall, J., Moura, I., Teixeira, M., Xavier, A.V. and Moura, J.J.G. (1988) Proc. Natl. Acad. Sci. USA 85, 9378–9380.
15 Bruschi, M. (1976) Biochem. Biophys. Res. Commun. 70, 615–621.
16 Bruschi, M. (1976) Biochim. Biophys. Acta 434, 4–17.
17 Hormel, S., Walsh, B.C., Prickril, B.C., Titani, K., LeGall J. and Sieker, L.C. (1986) FEBS Lett. 201, 147–150.
18 Watenpaugh, K.D., Sieker, L.C. and Jensen, L.H. (1980) J. Mol. Biol. 138, 615–633.
19 Adman, E.T., Sieker, L.C., Jensen, L.H., Bruschi, M. and LeGall, J. (1977) J. Mol. Biol. 112, 113–120.
20 Frey, M., Sieker, L., Payan, F.,Haser, R., Bruschi, M., Pepe, G. and LeGall, J. (1987) J. Mol. Biol. 197, 525–541.
21 Bruschi, M. and LeGall, J. (1972) Biochim. Biophys. Acta 263, 279–282.
22 Diaz, D. (1987) Thesis, University of Moscow, Moscow.
23 Diaz, D., Erokhin, A.S., Berezin, I.V. and Yatsimirkii, A.K. (1987) Zh. Obsch. Khim. 57, 715–716.
24 Johnson, R.S. and Schachman, H.K. (1980) Proc. Natl. Acad. Sci. USA 77, 1995–1999.
25 Strickland, E.H. (1974) Crit. Rev. Biochem. 2, 113–174.
26 Krishnamoorthi, R., Markley, J.L., Cusanonovich, M.A. and Przysiecki, C.T. (1986) Biochemistry 25, 50–54.
27 Werth, M.T., Kurtz, M.J., Moura, I. and LeGall, J. (1987) J. Am. Chem. Soc. 109, 273–275.
28 Moura, I., Teixeira, M., Xavier, A.V., Moura, J.J.G., Lespinat, P.A., LeGall, J., Berlier, Y.M., Saint Martin, P. and Fauque, G. (1987) Rec. Trav. Prat. Pays-Bas, 106, 6–7.
29 Lancaster, J.R. (1980) FEBS Lett. 115, 285–288.
30 Ballhausen, C.J. (1962) in Introduction to Ligand Field Theory, McGraw Hill, New York.
31 Kruger, H.-J. and Holm, R.H. (1990) J. Am. Chem. Soc. 112, 2955–2963.
32 Teixeira, M., Moura, I., Xavier, A.V., Nuynh, B.H., DerVartanian, D.V., Peck, N.D. Jr., LeGall, J. and Moura, J.J.G. (1985) J. Biol. Chem. 260, 8942–8950.
33 Van der Zwann, J.N., Albracht, S.P.T., Fontijn, R.D. and Slater, E.C. (1985) FEBS Lett. 179, 271–277.
34 Teixeira, M., Moura, I., Xavier, A.V., Moura, J.J.G., LeGall, J., DerVartanian, D.V., Peck, H.D., Jr. and Nuynh, B.H. (1989) J. Biol. Chem. 264, 16435–16450.
35 Alvarez, S. and Hoffmann, R. (1986) Anal. Quim. 82B, 52–56.
36 Rousset, M., Dermoun, Z., Hatchikian, E.C. and Belaich, J.P. (1990) Gene 94, 95–101.
37 Reeve and Beckler, (1990) FEMS Microbiol. Rev. 87, 419–424.
38 Voordouw, G., Menon, N.K., LeGall, J., Choi, E., Peck, H.D., Jr. and Przybyla, A.E. (1989) J. Bacteriol. 171, 2894–2899.
39 Shimizu, F., Ogata, M., Yagi, T., Wakabayashi, S. and Matzubara, H. (1989) Biochimie 71, 1171–1177.